Geopersia **7** *(1), 2017, PP. 35-54* *DOI: 10.22059/geope.2017.207609.648289*

Paleoenvironment, Biostratigraphy and sequence stratigraphic studies of the Permian-Triassic boundrary of the offshore Persian Gulf, Iran: using an integrated approach

Mina Mazaheri Johari [1*], Ebrahim Ghasemi-Nejad [2]
[1] *Research Institute for Earth Sciences, Geological Survey of Iran, Tehran, Iran*
[2] *Department of Geology, Faculty of Science, University of Tehran, Tehran, Iran.*
**Corresponding author, e-mail: m.mazaheri.pal@gmail.com*
(*received: 31/12/2016 ; accepted: 29/04/2017*)

Abstract

Four "supergiant" and numerous giant gasfields have been discovered in the Zagros area of SW Iran. The gasfields are concentrated in the eastern part of the simply folded belt and produce from Permo-Triassic carbonates belong to the upper member of the Dalan Formation and the overlying Kangan Formation. This boundary definitely plays a key role on reservoir quality and its impact exceedingly has highlighted the importance of studying on the boundary attributes. In this research a detailed biostratigraphic, microfacies and sequence stratigraphic study of the late Middle Permian to Early Triassic successions was undertaken from 850 thin sections prepared from cutting chips of well SPD12C-08 in South Pars Gas Field. Comparisons done with traditional Lopingian reference sections, allow sub-dividision of the Permian part of the studied deposits into four main biozones: 1) The late Midian is characterized by the FAD and the LAD of *Shanita amosi.* 2) The early Wuchiapingian is characterized by the FAD of *Paraglobivalvulina mira* during a first flooding event, strongly restructuring the Middle Permian habitats. 3) The "middle" Wuchiapingian is defined with the appearance of the genus *Paradagmarita monodi* and numerous regional markers. 4) The late Wuchiapingian is characterized by an assemblage dominated by *Charliella altineri* and *Neomillerella mirabilis*. The Triassic strata were all included in *Spirorbis phlyctaenae* Zone. Comparing the differentiated biozones with Tethyan zonation an age of Late Midian-Late Djulfian and Anisian is confirmed for the Dalan-Kangan formations, respectively. Dorashamian and Scytian deposits were not determined and that is a gap between the two formations. Microfacies studies led to the identification of 11 microfacies related to five facies belts. The general palaeogeographic context of this system was a marginal marine shelf setting with an inner platform that was very flat, ramp-like, with little topography but with local depressions. Indeed, four depositional sequences within several 3rd order cycles have been recognized.

Keywords: *Biostratigraphy, Depositional Environment, Sequence Stratigraphy, Dalan, Kangan, South Pars Gas Field.*

Introduction

The south Pars Gas field, the largest offshore field in the world, is located on the Iran-Qatar border in the Persian Gulf and also is shared by the two countries. This field -by the NNE-SSW trend- is part of the Pars/Qatar great dome. The Dalan (Djulfian age) and Kangan (Anisian age) formations are the most important reservoir rocks in this field and contain P-T boundary.

The evolution of life on Earth has been interrupted by mass extinction events at least five times. One of them, the largest of all mass extinctions, called Permian–Triassic event (251Ma), witnessed the loss of about 95 percent of species according to reverse rarefaction analysis (Raup, 1979; Vajda *et al.*, 2007). Therefore, this study is focused on detail biostratigraphy, paleoenvironmental and sequence stratigraphy analysis and precise definition of the depositional pattern at Dalan to Kangan interval in South Pars Gas Field, south of Iran.

Geological setting and stratigraphy

The South Pars Gas Field is actually the northern extension of the North field, located in the south of Iranian land in the Persian Gulf (Fig. 1). The Dalan and Kangan formations are the main reservoir of this field and are correlatable with upper part of the Khuff Formation in south of the Persian Gulf (in the Arabian plate) (Alsharhan & Nairn 1997; Kashfi 2000) (Table 1). The Dalan Formation has been assigned to the Middle to Late Permian and is subdivided into three members including Nar, K4, and K3, from bottom to the top, respectively (Fig 2). These consist of limestone, dolomite and some anhydrite layers. The Kangan Formation has been assigned to the Early Triassic (Szabo & Kharadpir 1978), and is subdivided into two members including K2 and K1. These members also consist of limestone, dolomite, anhydrite and mudstone (Fig. 3). The global P-T Boundary event is recorded within the K3-K2 transition (RahimpourBonab *et al.*, 2009).

Table 1. Details of Permian–Triassic rock units in South Pars Gas Field, Modified from Rahimpour-bonab *et al.*, 2009.

Chronostratigraphy				formations North	formations South	Reservoir
Triassic	Early	Anisian		Aghar Shale	Sudair Shale	
				Kangan	Upper Khuff	K1
		Scythian ?				K2
Permian	Late	Dorashamian ?		Upper Dalan		K3
		Djulfian	Upper?			
			Lower?			K4
	Middle	Morghabian		Nar Member	Middle Anhydite	
				Lower Dalan	Lower Khuff	K5-7
	Early			Faraghan	Haush-Unayzah	

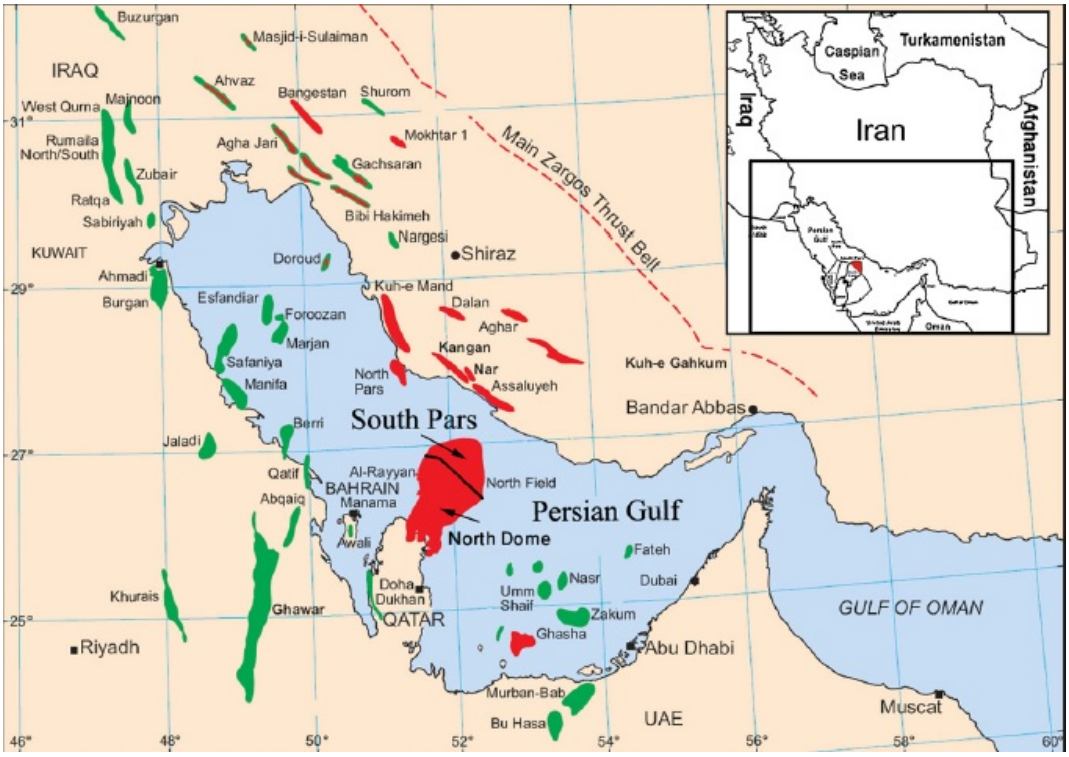

Figure 1. Geographical setting of the South Pars Gas Field. Main hydrocarbon fields in Persian Gulf and adjacent areas are shown (Modified from Insalaco *et al.*, 2006).

Material and methods

To investigate and xamine the P-T boundary in this study, core samples from one well covering the Permian – Triassic transition were examined thoroughly. This core interval consists of nine cores with a total thickness of 451.7 meter. Approximately 850 thin sections cut from horizontal plug samples (taken approximately every 30cm for conventional core analysis) performed by RIPI core lab were studied in detail. For biostratigraphy analysis, these thin sections were studied via using a polarized microscope, and for facies analysis, Dunham texture scheme was used together with sedimentary structures and fabrics, grain size, and diagnostic allochems such as ooids, pelloids, oncoids and shells. In addition, for reconstruction of the depositional environments classification of Flugel (2010) was used.

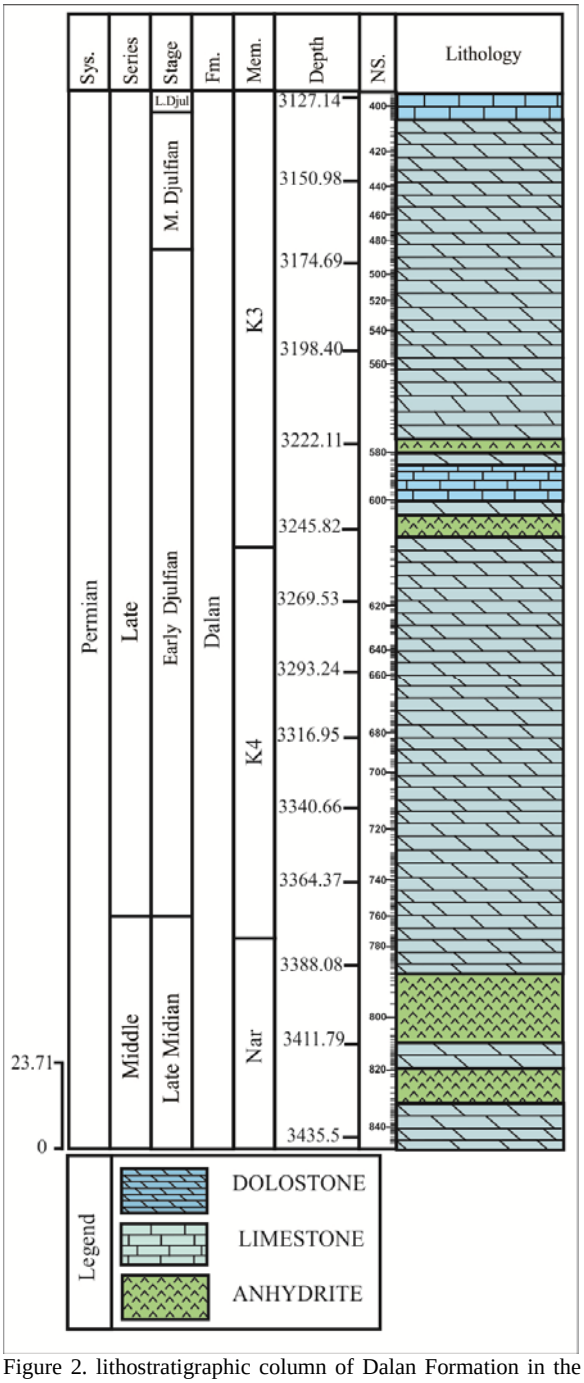

Figure 2. lithostratigraphic column of Dalan Formation in the South Pars Gas Field.

Disscusion

Biostratigraphy

Diverse and rich assemblages of foraminifera were recorded from different areas of the Tethyan basin. (e.g.: Mohtat *et al.*, 2005; Gaillot and Vachard, 2007; Rahimpour *et al.*, 2009; Gaillot *et al.*, 2009; Koehrer *et al.*, 2010; Vachard *et al.*, 2010; Song *et al.*, 2007, 2011; Kolodka *et al.*, 2011).

In this study, 95 species belonging to 49 genera of benthic foraminifera and 6 algal species (including *Permocalculus* sp., *Vermiporella* sp., *Pseudovermiporellasodalica*, *Mizziavelebitana*, *Permocalculus solidus* and *Pseudoepimastoporalikana*) have been identified and their stratigraphic distribution were drawn (Fig. 4). Based on these data, five biozones were erected and correlated to the other parts of the Tethyan basin (Table 1, 2). These biozones include:

Shanita amosi Range Zone

This zone spans from the FO to LO of *Shanita amosi*, and is equivalent to *Shanita amosi* Zone of Gaillot and Vachard (2007), *shanita* Zone of Kolodka *et al.* (2011) and *Reitlingeria* Zone of Mohtat *et al.*, (2005). The index species *Shanita amosi* is a marker for Late Midian stage (Dawson *et al.*, 1993, 1994; Insalaco *et al.*, 2006). The FO and LO of *Shanita amosi* was recorded at 3438- 3427.5 m respectively (Dalan Fm., Table 2). This biozone is overlain by the *Paraglobivalvulina mira* Range Zone (Early Djulfian).

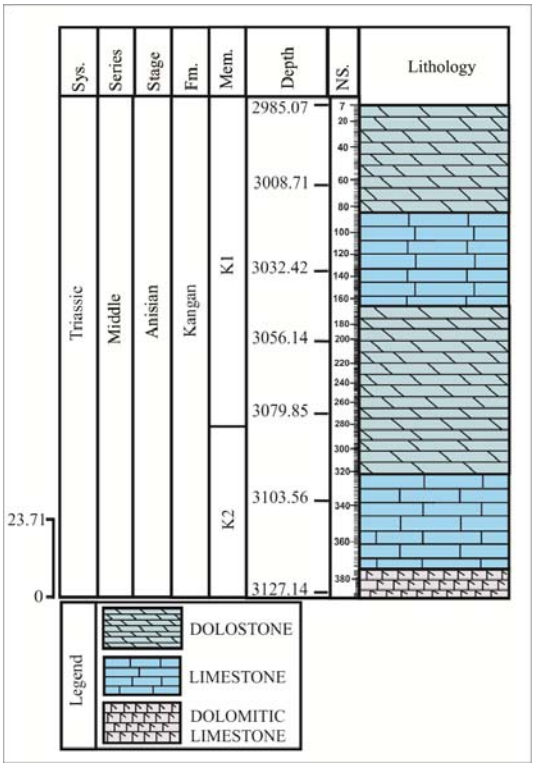

Figure 3. Lithostratigraphic column of the Kangan Formation in the South Pars Gas Field.

Table 2. Correlation of the benthic foraminifera biozonation of the Dalan Formation with other studied sections in Tethys basin.

Formation	Stage	Zagros basin, Southwest Iran	Turkey and South China	Northwestern Turkey	Northeastern Iran	Tethyan area	This Study
		Baghbani, D.1372	Gaillot, J & Vashard, D.2007	Leven, 1991	Lys, Stamply & Jenny, 1978	Leven, 1981	
Dalan	Late Djulfian	*Rectostipulina* Zone	*Charliella altineri* Zone	*Gabeina* Sp./ *Lepidolina* Sp. Zone	*Codonofusiella nana*/*C.luishang Zone*	*Reichelina* Zone	*Charliella altineri* Interval Zone
	Middle Djulfian		*Paradagmarita monodi* Zone				*Paradagmarita monodi* Range Zone
	Early Djulfian		*Paraglobivalvulina mira* Zone				*Paraglobivalvulina mira* Range Zone
	Late Midian	*Shanita* Zone	*Shamita amosi* Zone	———	———	*Yabeina/Lepidolina* Zone	*Shamita amosi* Range Zone

Paraglobivalvulina mira Range Zone

This zone spans from the FO to the LO of *Paraglobivalvulina mira*, and is equivalent to Zone No.4 (*Dagmarita shahrezaensis* and *Frondina permica*) and Zone No.5 (*Reichelina*) of Mohtat *et al.*, (2005), *Paraglobivalvulina mira* Zone of Rahimpour *et al.* (2009), and *Paraglobivalvulina mira* Zone of Kolodka *et al*. (2011). In addition, *Labiglobivalvulina fortis*, *Frondina permica*, *Dagmarita chankchiensis*, and *Nankinella* sp. species were present in this zone. Based on such index species as *Frondina permica* an age of Late Permian (Early Djulfian) was assigned to this zone. The FO and LO of *Paraglobivalvulina mira* was recorded at 3375.09- 3171.15 m respectively (Dalan Fm., Table 2).

Paradagmarita monodi Range Zone

This zone spans the FO to the LO of *Paradagmarita monodi*, and is equivalent to *Paradagmarita monodi* Zone of Gaillot & Vachard (2007). *Nodosinelloides mirabilis* and *Pachyphloia* sp. were associated species. The zone is assigned to Late Permian (Middle Djulfian) and the FO - LO of *Paradagmarita monodi* was recorded at 3171.15-3130.05 m respectively (Dalan Fm., Table 2).

Charliella altineri Interval Zone

This zone spans from the FO of *Charliella altineri* to the FO of *Spirorbis phlyctaenae* species, and is equivalent to *Charliella altineri* Zone of Gaillot & Vachard (2007).

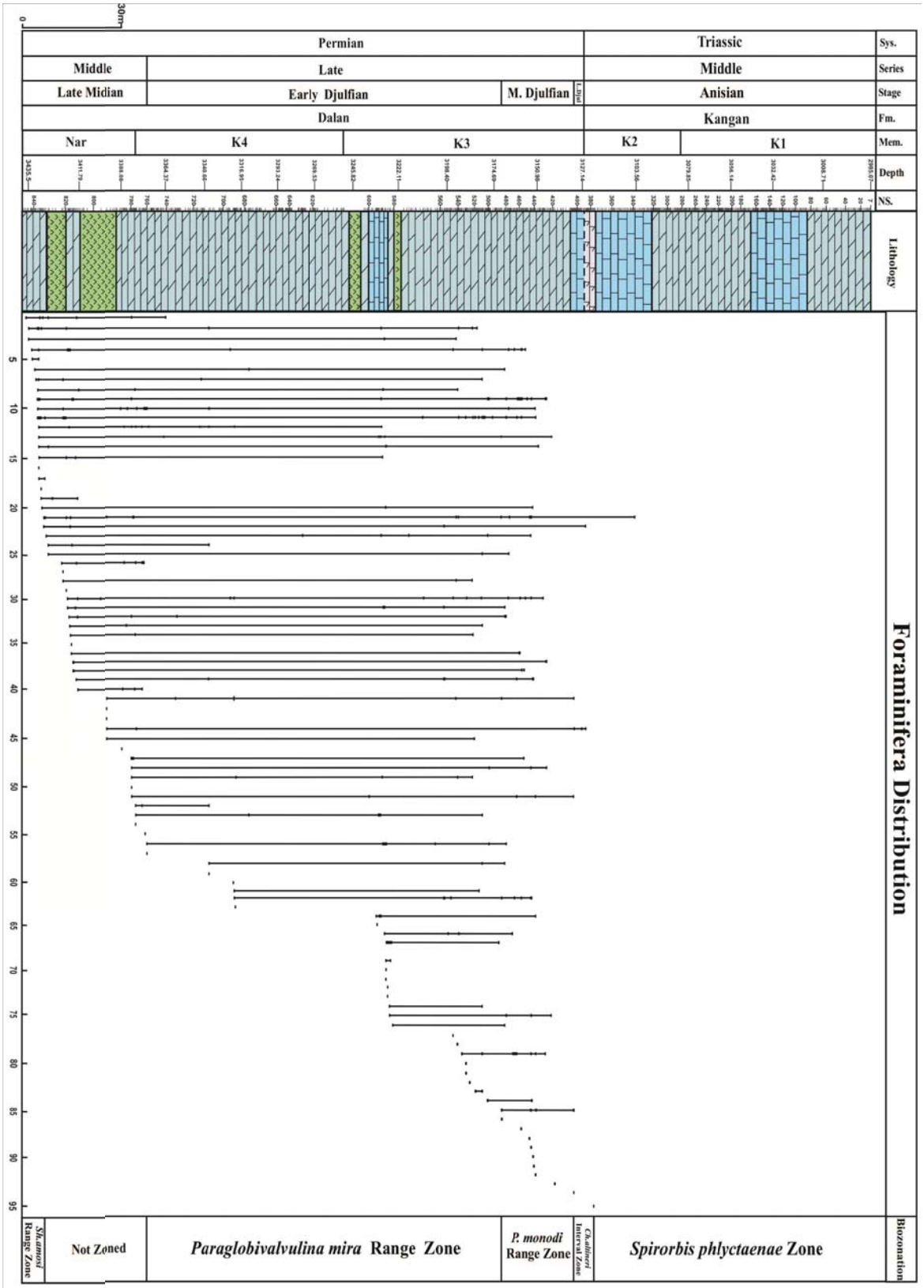

Figure 4. Stratigraphic distribution of benthic foraminifera in the Permian-Triassic at the South Pars Gas Field.

The *Neomillerella mirabilis* species which is considered as index species for Late Djulfian (Insalaco *et al.*, 2006; Gaillot&Vachard, 2007) was accompanied with other Late Djulfian index forms such as: *Dagmarita chanackchiensis*, and *Paraglobivalvulina mira*. This zone is therefore, given an age of Late Permian (Late Djulfian). The FO of *Charliella altineri* species and the FO of *Spirorbis phlyctaenae* species was recorded at 3130.05- 3120.25 m respectively (Dalan Fm., Table 2).

***Spirorbis phlyctaenae* Range Zone**

This zone spans from the FO to the LO of *Spirorbis phlyctaenae* and is equivalent to *Spirorbis phlyctaenae* Zone of Zaninetti (2004) and *Ammodiscus parapriscus*/*Glomospirella facilis* Zone of Bronniman & Zaninetti (1972). This interval is dated Anisian (Middle Triassic) based on the presence of *Spirorbis phlyctaenae*, the index species for this stage. The FO of *Spirorbis phlyctaenae* species was recorded at 3120.25 m and continuous to the top of the section (Kangan Fm., Table 3).

Microfacies and depositional environment

The facies described and interpreted have been classified in terms of overall depositional environment including: 1) sabkha 2) intertidal 3) restricted lagoon 4) huge oolithic to bioclastic shoal bodies and 5) open marine areas (Fig. 5). In general, Palaeoenvironmental context of this system was a marginal marine shelf setting with an inner flat platform, ramp-like, with little topography but with local depressions as could be concluded from the microfacies differentiated.

Eleven distinctive microfacies were characterized and differentiated by different texture and sedimentary environments. A summarized description of these core facies is given below:

MF1: Heavily Bioturbated Mudstone

The core facies is mainly characterized by heavily bioturbated mud-supported facies. There are some bioclastic debris including echinoid fragments, sponge spicules and small foraminifers (Fig 6, MF1).

Bioturbated mudstones and wackstones are interpreted as open-marine deposits of a low-energy setting (deepest parts of Inner ramp). This environment is characterized by strongly varying oxygen levels, reduced circulation and low sedimentation rates (Koehrer *et al.*, 2010). This facies exhibits a mottled appearance that created by heavily bioturbation and trace fossils (such as Zoophycus, Planolites and Rhizocorallium). Based on the mentioned description it seems that this particular facies had a close relationship to sea level rising and changes in carbonate sedimentation rate. This facies type may correspond to facies type F11 of Insalaco *et al.* (2006).

MF2: Oolitic Grainstone (ooidal dolograinstone)

In this core facies the dominant allochems are oolites (although significant amounts of peloid, bioclasts and lithoclasts can be present). This facies is characteristic of shoal or Sand Island environments (Koehrer *et al.*, 2010). Ooids (The concentric (tangential) ooids are dominant) are more abundant than other grains (> 90%) (Fig 6, MF2). These are evidences of high energy conditions in a depositional environment together with tidal regime. It is probably equivalent to facies RMF 29 of Flugel, 2010.

MF3: Ooid (Oncoid) Bioclast Grainstone

These deposits generally consist of ooid, oncoid and bioclasts grains (such as: bivalves, crinoids, bryozoans, and calcareous algae), and less pellet and intraclast.

Table 3. Correlation of the benthic foraminifera biozonation of the Kangan Formation with other studied sections in Tethys basin

Formation	Age	Upper Triassic Carbonate deposits of Indonesia	In Triassic rocks of Europe and Iran	This Study
		Zaninetti, 2004	Bronniman, Zaninetti,1972	
Kangan	Anisian	*Spirorbis phlyctaenae* Zone	*Ammodiscus parapriscus/ Glomospirella facilis*	*Spirorbis phlyctaenae* Zone

The bioclast grains have often big size (sometimes about 2mm) (Fig 6, MF3). This depositional setting is ranged from lower intertidal environment to lagoonal shoal margin setting (leeward) located within an internal platform context with moderate to high energy condition (Flugel, 2010). This is probably equivalent to facies RMF 26 of Flugel, 2010.

MF4: Pel Ooid Grainstone

This microfacies is very similar to the previous one. Although ooids are still the dominant allochem, the major difference with MF3 is in relative increase of pelloids. The main components are pelloids and ooids (Fig 6, MF4). These are deposited in the nearest environment to lagoon relative to the previous facies (Flugel, 2010).

MF5: Intraclast Peloidal Grainstone

These peloidal deposits contain abundant pelloids and intraclasts, and rare ooids and bioclasts (such as: benthic foraminifera and algae) (Fig 6, MF5). Foraminifera are common and show a low to moderate diversity with large miliolids, nodosariids, and biseriamminids. Thick intervals of massive pelloidal grainstones are especially recognized within the Upper Permian section (Koehrer *et al.,* 2010).

This facies was located in outer part of the lagoon (lagoon- shoal transitional zone) with moderate to high energy condition, and in some cases could reflect relatively well sorted beach ridge (shore face). They are often intercalated with muddy and oolithic facies as the system exhibits a significant lateral changing to muddy lagoon or oolithic shoal settings (Flugel, 2010).

MF6: Bioclast Ooid Packstone to Wackestone

The remarkably variety of allochemes is the most important feature of this microfacies. These deposits essentially consisting of bioclasts (such as: crinoids, ostracods, gastropods calcareous algae, and bivalves) and ooids. It should be mentioned that in some cases these allochemes appear as grain-supported and some others as mud-supported (fig 6, MF 6 Increase in ostracods, gastropodes and widespread presence of pelloids and intraclasts with appearance of micritic facies are the evidences of a lagoon environment in the carbonate ramp system. This might be equivalent to facies RMF 20 of Flugel (2010).

MF7: Pelintraclast Packstone to Wackestone

Although pelloid and intraclasts are still the major grains in this wackestone-packstone microfacies, the presence of skeletal debris including gastropods and bivalves have been decreased and their frequency are rare (fig 6, MF7).

As it is mentioned, these deposits are mainly consisting of pelloids and intraclasts and increasing of pelloid grains can be a reliable evidence to quoting a lagoonal depositional system to this microfacies (Insalaco et al., 2006, Flugel, 2010). The related microfacies is equivalent to facies RMF24 of Flugel (2010).

MF8: Mudstone

Once again the micritic mud is dominated in this microfacies and benthic foraminifers can be rarely seen (small foraminifers often show a darker color in the thin section). Although the sparse intraclasts have observed, the allochemes frequency is less than one percent. In comparison with the first microfacies (MF1) the bioturbation event is not recorded in this microfacies (fig 6, MF8).

This microfacies suggest deposition in a lagoonal and intertidal environment and is equivalent to facies RMF 22 of Flugel (2010).

MF9: Anhydrite fenestral Mudstone

These are essentially muddy facies with significant indications of intertidal influences. This facies contains anhydrite nodules and fenestrate texture (fig 6, MF 9). These evidences are indicators for hyper saline, sabkha and upper part of intertidal environments (Shin, 1983). This facies is equivalent to facies RMF 25 of Flugel (2010).

MF10: Thrombolitic- StromatoliticBoundstone

This microfacies is deposited in shallow upper subtidal lower intertidal environments (Fig. 6, MF 10). The Thrombolitic facies developed within a pocket of high energy intraclastic sediments and also is interpreted as shallow subtidal to intertidal stromatoitic/thrombolithic patches in lower energy conditions (upper subtidal setting), and encrusted firmly by stromatolite algal mats (Grotzinger, 2000). The abundant lithoclastic material found around the thrombolitic interval is due to reworking under progressively storm-wave conditions just after Permian/Triassic stratigraphic disconformity (Insalaco *et al.,* 2006). This facies is equivalent to facies RMF 23 of Flugel (2010).

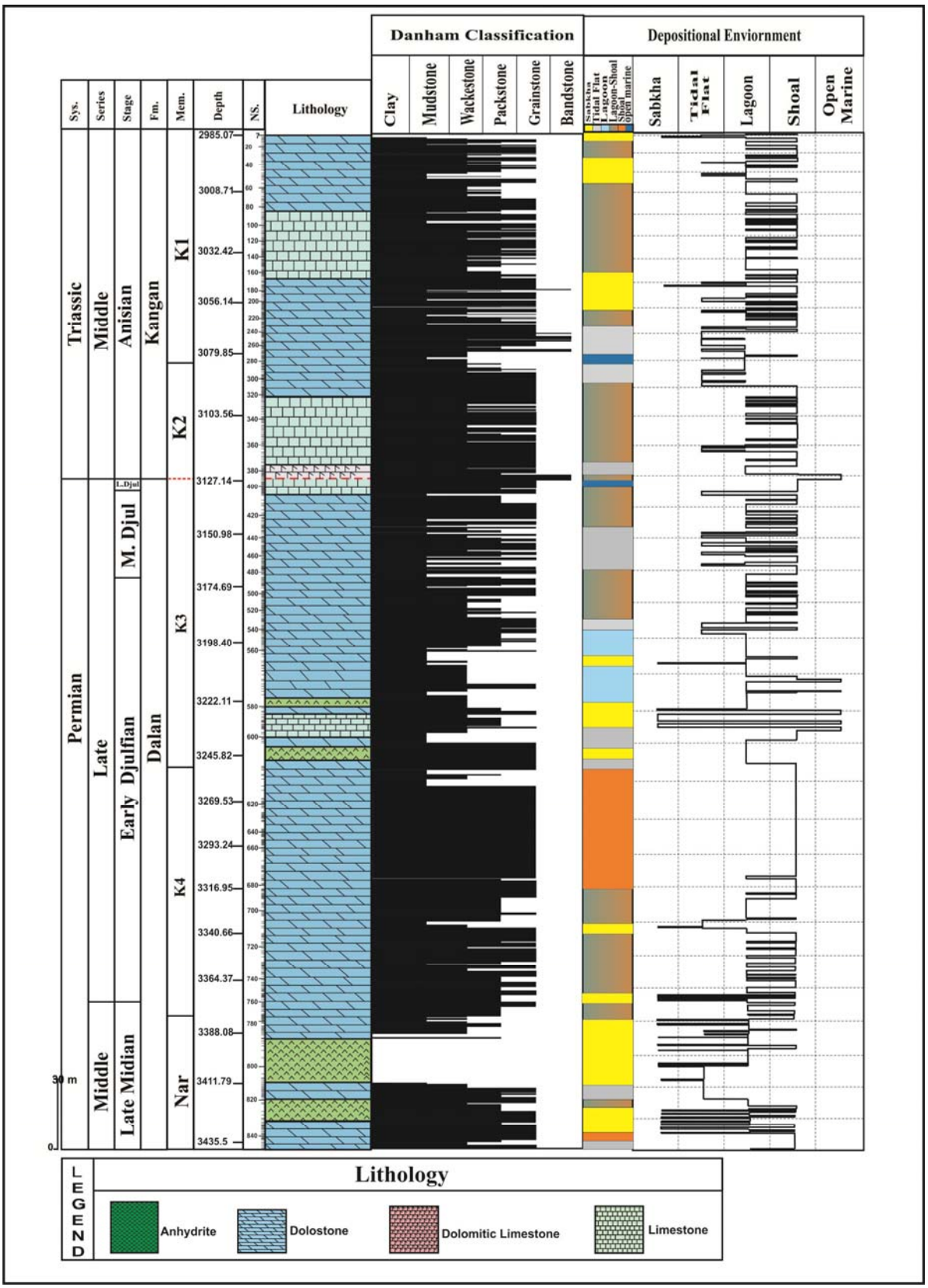

Figure 5. Stratigraphic column, Depositional environment, and facies types of the studied formations

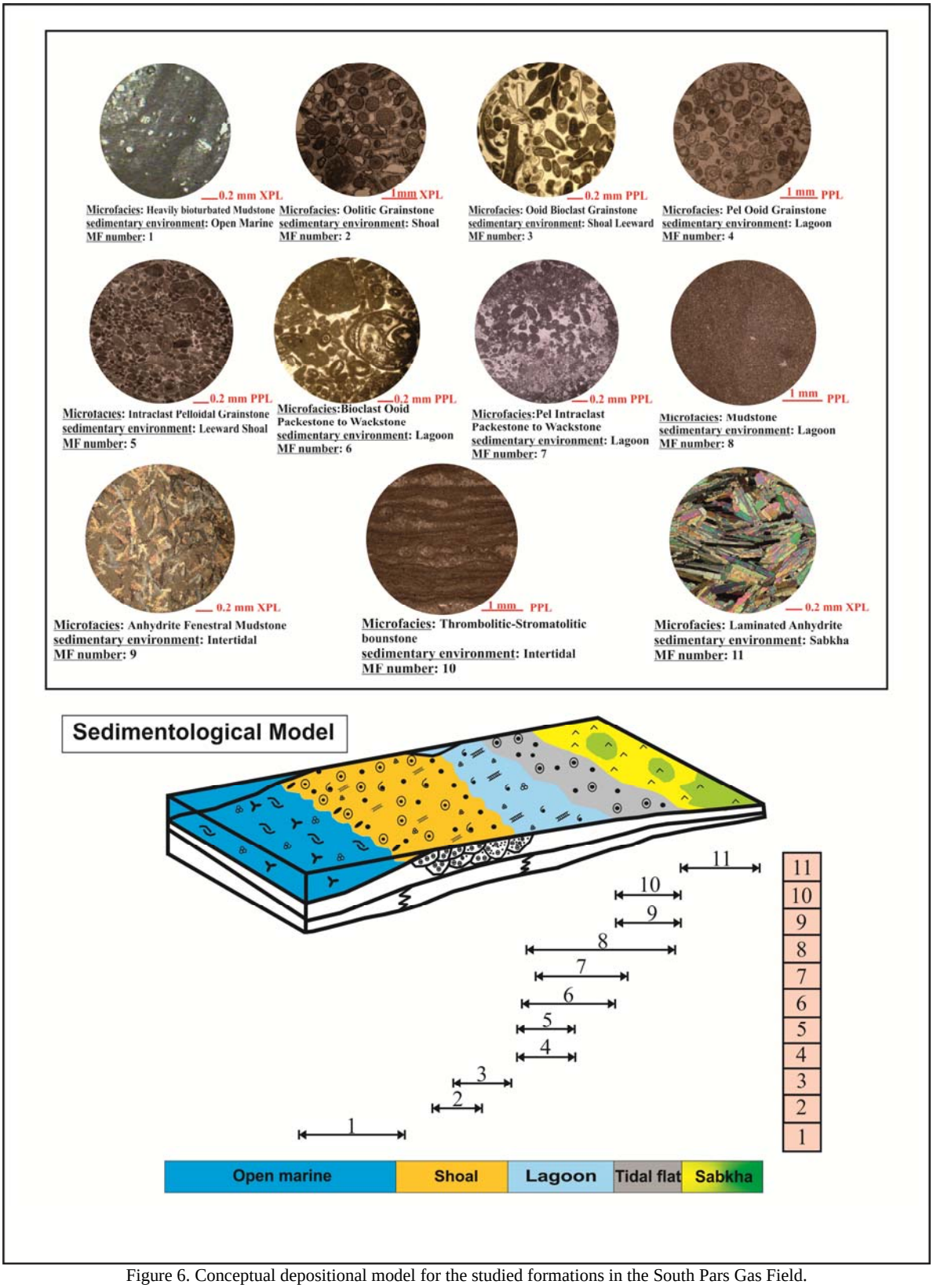

Figure 6. Conceptual depositional model for the studied formations in the South Pars Gas Field.

MF11: Laminated Anhydrite

The anhydrite in this fabric shows a variety of forms bedded to massive, finely laminated and nodular fabrics. This microfacies could have developed as both supertidal sabkha type deposits and shallow coastal facies (Rahimpour-Bonab *et al.,* 2009). With the absence of clear evidence of selenite pseudomorphs the interpretation of salina is more equivocal and speculative. The fact that these subtidal evaporates are subsequently sabkha aired (due to the very low accommodation space) means they are effectively turned to sabkhas (salina) (Rahimpour-Bonab *et al.,* 2009). An additional complication is the presence of secondary anhydrites resulting from anhydritization of carbonates. Based on the aforementioned depositional facies, a depositional model was established for the Dalan- Kangan formations (Fig. 6). According to this model which is similar to those proposed for carbonate platforms by Sharland *et al.* (2001) and Stampfly (2000), these formations were deposited in a carbonate ramp (Fig. 7). Additional evidences for this conclusion includes:
Absence of big riff structure.
Absence of oncoids, pisoids, and aggregate.
The lack of slid/slump facies.
The lack of turbidities facies.
Gradual changes of facies to each other. Significant changes in platform sedimentation from the K1 through to the K4 have been recorded. Consequently, different depositional models were proposed for each of the major stratigraphic intervals (Figures 8 to 9).

Depositional models of K1 & K2 units (Kangan Fm.)

K1: This depositional unit is dominated by peritidal and evaporitic supratidal flats with pervasive microbial facies. This is also a zone of small shoal development. This unit consists of dolomite, anhydrite dolomite, limestone, and is deposited in a sabkha and tidal environment as mentioned above.

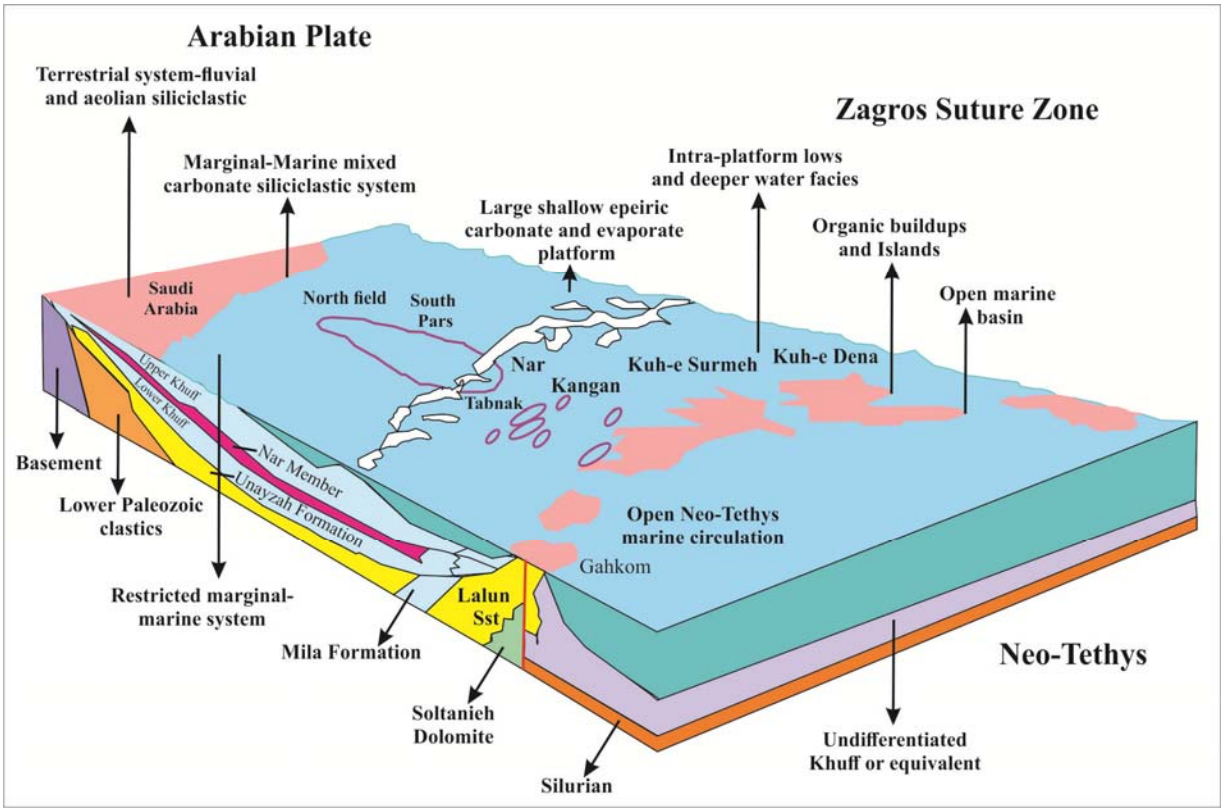

Figure 7. Conceptual paleogeographic model for upper Dalan- Kangan carbonate ramp in the Persian Gulf Basin (Stampfly, 2000; Sharland *et al.,* 2001).

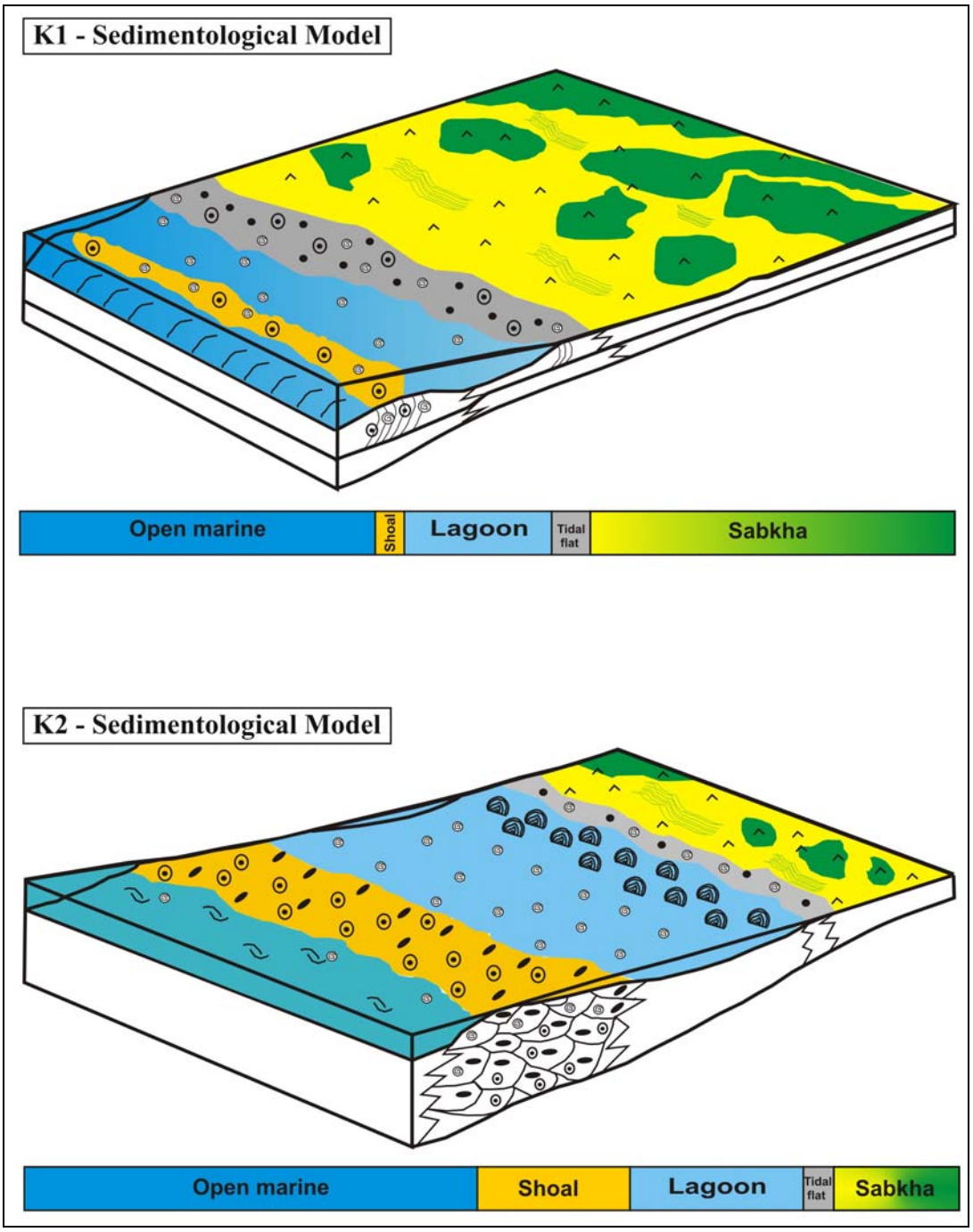

Figure 8. Conceptual depositional model for the K1 and K2 units of the Kangan Formation.

However, from the K1 through to the K2 there have been significant changes in platform sedimentation, facies associations and climate, consequently different depositional models need to be created for each of the major stratigraphic intervals (Fig. 8, A).

K2: This unit is dominated by dolomite (upper part) and limestone (lower part), although the anhydrite portion has relatively decreased in comparison with the K1 unit. The K2 unit is composed of grainy aggradational facies and local mudstones. Regarding expansion of pelloids, intraclasts and euryhaline organisms such as ostracods, gastropods and some special genesis of algae, a lagoonal environment is the indicative sedimentary environment in this unit. It is necessary to mention

that this facies include beach and shallow-water thrombolitic facies followed by storm generated pebble grainstone beds and shoals, which have varying degrees of microbial influence (Fig. 8, B).

Depositional models of K3 & K4 units (Dalan Fm.)

K3: This unit is mainly composed of dolomite, but in the upper and lower parts have different lithology such as: Anhydrite, limy-dolomite, dolo-limestone, marly limestone and limestone. Based on this study, the K3 is a system composed of restrictive coastal lagoons and shallow-water muddy facies associated with some tongues of outer ramp facies (Fig. 9, C). It should be mentioned that development of lagoonal environment in the K3 is more than K2 unit. In contrast shoal extension in this unit is less dominated than in the previous unit (K2).

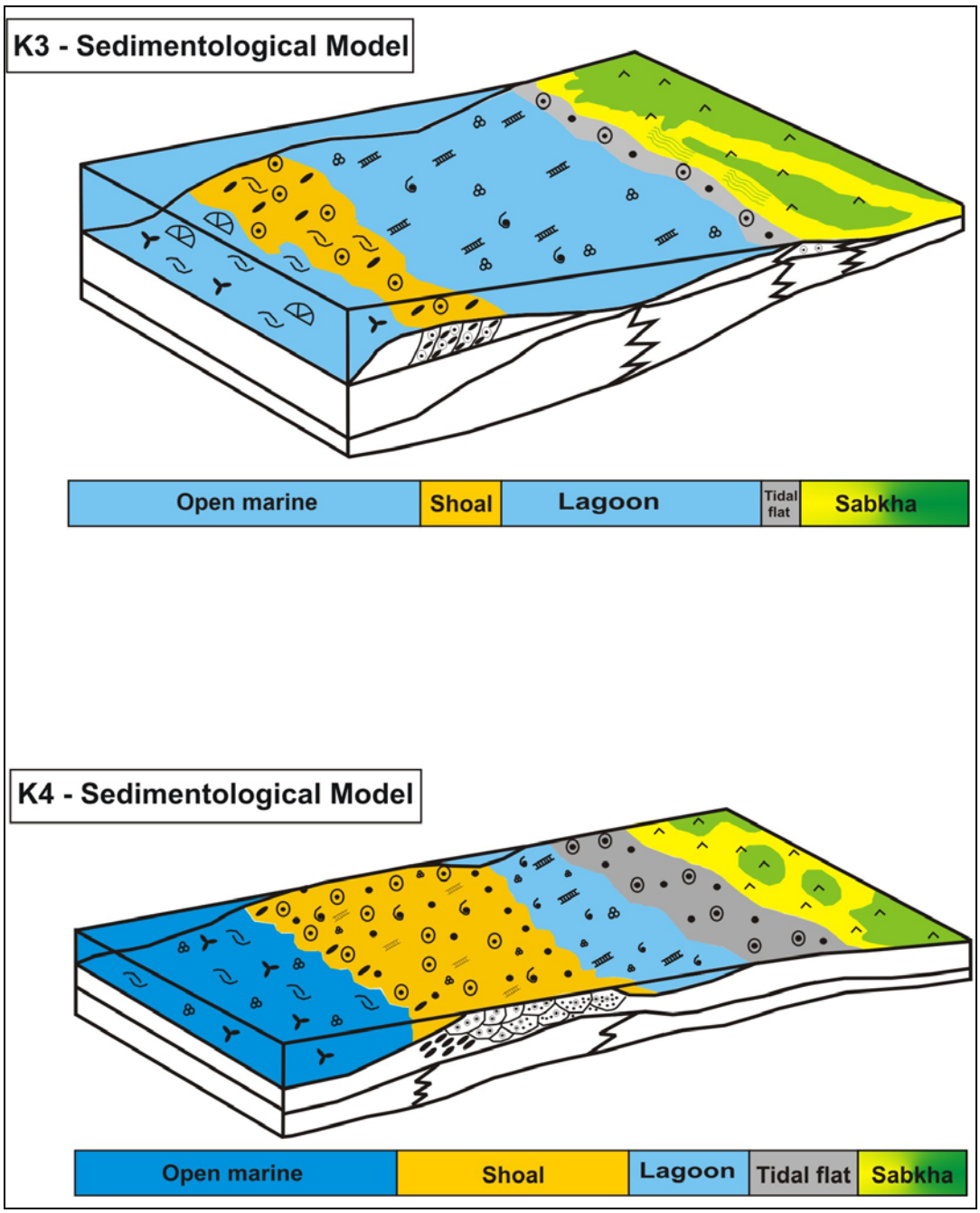

Figure 9. Conceptual depositional model for the K3 and K4 units of the Dalan Formation.

K4: This unit is composed of dolomite and limestone (grainstone based on Dunham classification). The K4 equates to huge subtidal bioclastic and oolitic shoals with local lagoons. The reservoir sector of this unit is mainly composed of bioclastic and oolitic transgressive sand wave complexes, which are preceded by a thin muddy "open" interval and finally capped by internal restricted platform conditions. The shoal depositional environment of this unit is more dominant than the other units (Fig. 9, D).

Sequence stratigraphical analysis

A high resolution sequence stratigraphy has been accomplished on Kangan Formation and upper part of the Dalan Formation in order to distinguish the major cycles, preliminary sedimentary basin analysis in the field (Fig. 10).

Four distinct composite sequences and eight depositional sequences were differentiated through the core interval, which have included several smaller cycles, system tracts and parasequences. The typical system tracts have been recognized in the core intervals including transgressive and highstand systems tracts that were deposited on the carbonate platforms causing frequent sea level fluctuations. There is no evidence of any clastic deposits, due to the lack of any silisiclastic or long term sub-aerial exposure.

However, the above mentioned successions were bounded by several distinctive sequence boundaries with significant sub-aerial exposure (SB type2) that separated the depositional sequences. The MFS key beds have been identified using the parameters such as lithology, biostratigraphy, sedimentology and sequence stratigraphy interpretations. The MFS key beds were placed generally between deepening-upward transgressive system tract and shallowing-upward highstand systems tracts. Therefore, the nomenclature of the sequence stratigraphic subdivisions presented in this study is KS1 to KS4, which have covered K1 to K4 units and they are described below.

Upper Dalan KS4 Depositional sequence

The KS4 composite depositional sequence has been subdivided into two major intervals or 3rd order sequences: the KS4a at the base and KS4b at the top. These two sequences comprise various depositional units.

KS4a sequence

The overall transgressive-regressive cycle of the KS4a (i.e. from the top Nar surface to the major dolobreccia surface (major SB) at the top of the KS4) can be assimilated into 4th order transgressive-regressive stacking pattern.

The base of this depositional sequence is composed of a series of dolomitic mud supported facies such as bioclast/peloid wackestone to packstone and some layers of anhydrite. The following cycles become progressively more grain supported, including oolitic/pelloidal grainstones with bioclasts. This cycle marks the start of the fining-upward, grainstone-dominated, and mudstone capped thin depositional cycles.

KS4b Depositional sequence

The KS4b is a third order depositional cycle, which usually is dominated by well-developed oolithic facies and this sequence is the thickest cycle within the KS4 mega cycle set. This sequence is mainly characterized by aggradational stacking pattern. This depositional sequence started with series of fining-upwards oolitic/peloidal grainstones, with tidal flat to lagoonal mud supported facies in the upper parts. There is a well-developed fine to medium grained bioclastic pelloidal grainstone at the top of this depositional unit that belongs to lower intertidal environment and relatively thick anhydrite layers.

Upper Dalan KS3 Depositional sequence

The KS3 composite depositional sequence has been subdivided into two major intervals or 3rd order depositional sequences: the KS3a at the base and KS3b at the top. The KS3a comprises various depositional units. It should be stressed that each major depositional sequence consist of a significant TST and HST sedimentary portions, which are characterized by retrogradational, aggradational and progradational stacking patterns.

Depositional units in KS3a

The overall transgressive-regressive cycle of the KS3a can be assimilated into 4th order transgressive-regressive stacking pattern. This depositional unit starts with a thick anhydrite bed with some interlayers of dolomitic and limy wackestone, grainstone, and mudstone.

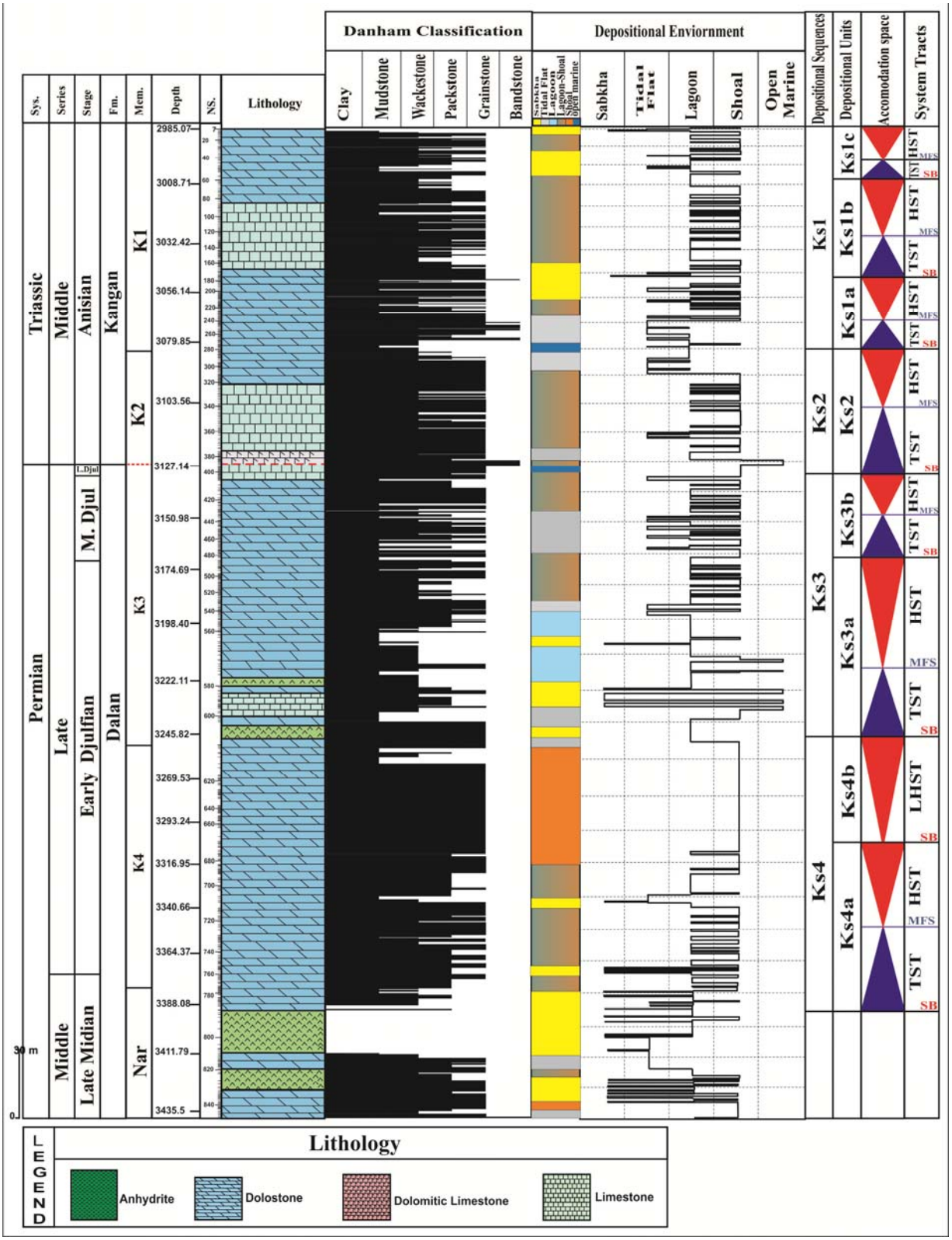

Figure 10. Stratigraphic column, depositional environment, facies types, and depositional sequences for the studied rock units.

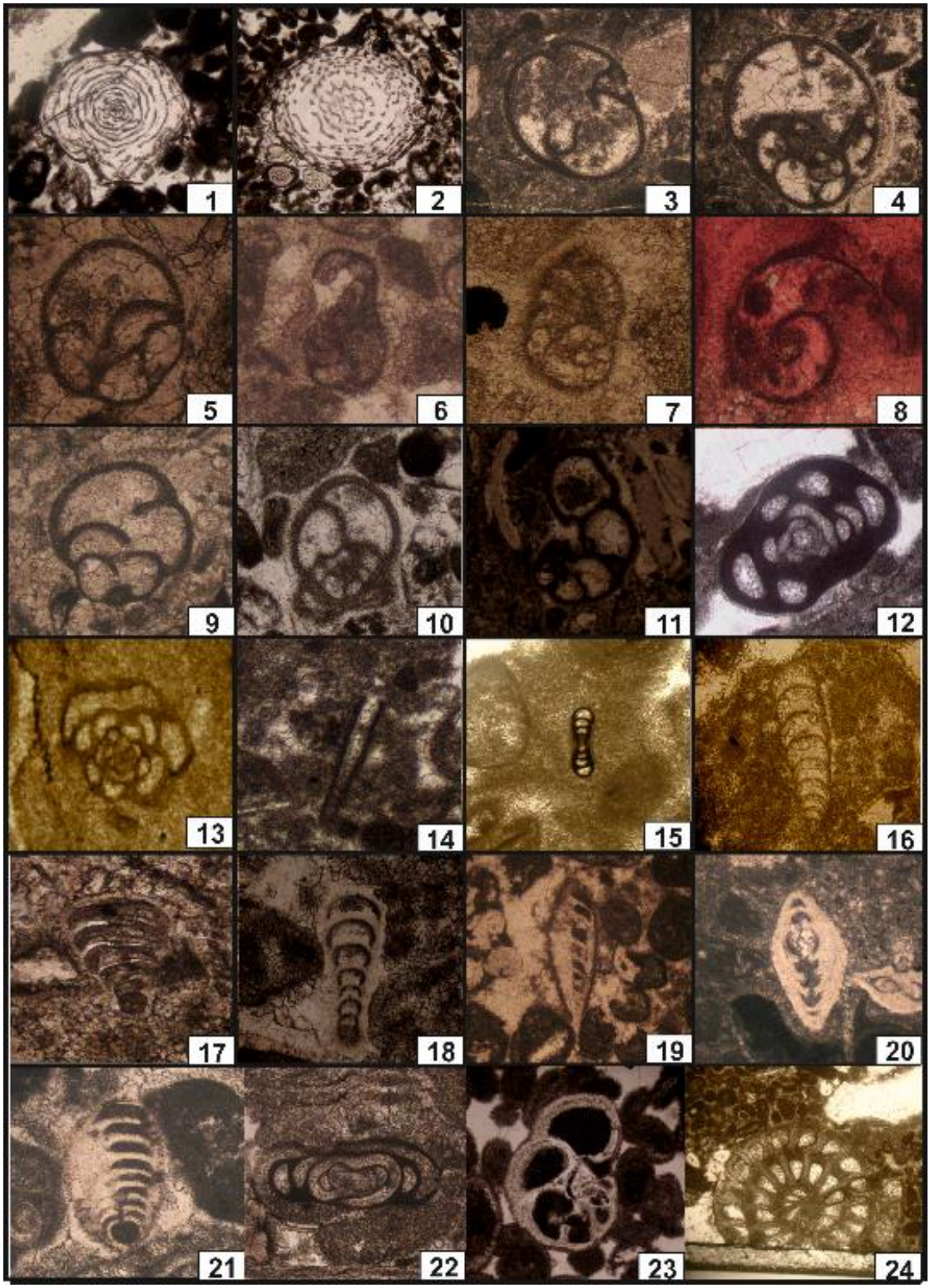

Plate 1. N.1-2: *Shanita amosi* Bronniman, Whittaker & Zaninetti, 1978, N.1 (32X; 3430.07 m), N.3 (16X; 3430.07 m), Dalan Formation, Age: Late Midian. N.3-4: *Paraglobivalvulina mira*, Reitlinger, 1965, All: 30X; 3228.71 m, Dalan Formation, Age: Dzhulfian. N.5: *Charliella altineri* Gaillot and Vachard, 2007, 75X; 3129.70 m, Dalan Formation, Age: late Wuchiapingian.nN.6-7: *Paradagmarita monodi* LYS *in* LYS & MARCOUX, 1978, N.6 (32X; 3171.15 m), N.7 (80X; 3151.52 m), Dalan Formation, Age: Changhsingian. N.8: *Spirorbis phlyctaena* Brönnimann and Zaninetti, 1972, 32x; 3120.25 m, Kangan Formation, Age: Anisian. N.9:

Labioglobivalvulina fortis, Gaillot and Vachard, 2007, 80X; 3314.14 m, Dalan Formation, Age: Lopingian. N.10: *Globivalvulina Vonderschmiti* Reichel-Whittaker *et al.*, 32X, 3229.25 m, Dalan Formation, Age: Early Julfian. N.11: *Globivalvulina bulloides* Brady, 1876, 32X, 3228.71 m, Dalan Formation, Age: Julfian. N.12: *Glomomidiella nestellorum* Gaillot and Vachard, 2007 (=Kamurana? SP. Nguyen Duc Tien, 1989), 70X, 3380.67 m, Dalan Formation, Age: Midian. N.13: *Hemigordinella regularis* Lipina,1949, 75X, 3425.94 m, Dalan Formation, Age: Changhsingian. N.14: *Earlandia elegans,* Rauzer-Chernousova & Reitlinger, 1937,32X, 3181.15 m, Dalan Formation, Age: Late Changhsingian. N.15: *Cornuspira kinkellini,* Spandel,1898, 75X, 3427.01 m, Dalan Formation, Age: Capitanian- Triassic. N.16: *Frondia permica,* Sellier De Civrieux & Dessauvagie,1965, 80X, 3380.67 m, Dalan Formation, Age: Lopingian. N.17: *Geinitzina postcarbonica,* Spandel, 1901, 75X, 3314.14 m, Dalan Formation, Age: Earliest-latest Permian. N.18: *Geinitzina reperta,* Bykova 1952, 80X, 3229.25 m, Dalan Formation, Age: Murgabian to Median. N.19: *Pachyphloia schwageri,* Sellier De Civrieux & Dessauvagie, 32X, 3151.52m, Dalan Formation, Age: Lopingian. N.20: *Pachyphloia enormis,* Gaillot and Vachard, 2007, 32X, 3228.71 m, Dalan Formation, Age: Late Midian- Lopingian. N.21: *Langella massei*, Gaillot and Vachard, 2007, 70X, 3229.25 m, Dalan Formation, Age: Late Changhsingian. N.22: *Agathamina* cf. *pusilla,* Geinitz in Geinitz & Gutbier,1848, 75X, 3167.42 m, Dalan Formation, Age: Wuchiapingian– Changhsingian. N.23: *Paremiratella robusta ,* Gaillot and Vachard, 2007, 80X, 3161.8 m, Dalan Formation, Age: Changhsingian. N.24: *Neoschwagerina simplex,* Ozawa, 1925, 24X, 3427.01 m, Dalan Formation, Age: Lower Murgabian.

The rest of the parasequence set is a series of dolomudstone to wackestone with inter layers of grainstone. The cycles developed in a restricted lagoonal/peritidal to open marine environment with occasional transgrasive peritidal to sabkha environments representing slightly low energetic conditions at the base of the cycles. The tops of the cycles represent intertidal mudflat and lagoonal environments. The maximum of accommodation occurs after the open marine setting within a restricted subtidal to peritidal facies and small shoal or bars.

Depositional units in KS3b

This is a 3rd order cycle located in the upper part of the upper Dalan member. This sequence represents significant shallowing upward cycle that corresponds to eustatic sea level falling during the Late Permian stage. This unit is started an exposure surface at the base and grain supported dolostone with big lag deposits that show flooding. High energy condition with lithoclast lag deposits to hyper saline lagoons and microbial mudflats developed at the base of the sequence. These are followed by bioturbated lagoons, tidal flat, and bioclastic lagoonal margin. At the top oolithic and bioclastic sands represent shallow subtidal to intertidal setting. The grainstones packs that are strongly erosional, rich in lithoclastic material may represent cannibalistic tidal channels. The lithified mudflats are common and reflect significant exposure of the mudflats to allow lithification and then erosion by either the following cycle or a tidal channel. The TST sediments are dolomitized with high percent of secondary anhydrite plugging.

Lower Kangan KS2 depositional sequence

The Triassic depositional sequences were deposited on the significant Late Permian disconformity and exhibit a transgressive sedimentation above the hiatus. The Kangan depositional sequence consists of four major third order cycles (KS2, KS1a, KS1b, and KS1c).

The KS2 depositional sequence starts with coarse intraclastic/oolithic grainstone with microbial features and oncoids. This grainstone cycle is composed of oolites, peloids, and bivalve bioclasts. This grainy cycle represents a significant flooding and opening-up of the platform system over the very internal muddy platform interior facies of the KS3b cycle. The upper part of these grain supported facies is characterized by microbial thrombolitic facies associated with clotted fabric. This is a very distinctive marker bed. Over the thrombolite boundstone facies grain supported facies is dominated along with the limy wackestone to packstone lagoonal facies. The upper part of the depositional sequence is characterized by dolomitic mudstone and mixture of oncoid/oolithic grainstone and bioclastic wackestone/packstone. Dolomitic mudstone/wackestone and stromatolite boundstone cap this sequence.

Upper Kangan KS1 Depositional sequence

The KS1 composite depositional sequence has been subdivided into three major 4th order depositional sequences; KS1a, KS1b, KS1c. This composite depositional sequence equates to the upper Kangan interval, which is characterized by pervasive evaporate sediments.

Depositional units in KS1a

This parasequence set is started with transgressive lag deposits and followed by alternation between anhydritic laminated stromatolite boundstone and oolithic grainstone. This alternation was continued by dolowackestone to packstone facies and few shale layers. Shallowing upwards cycles start after

these facies. In this depositional sequence upper intertidal to supratidal features are dominant, with evidence of microbial mats, upper intertidal muds, and supratidal facies.

Depositional units in KS1b

At the base of this sequence there is an anhydrite layer and traces of exposure surface. The TST starts with a well-developed series of lagoonal and tidal flat facies, consists of intercalated with microbial influenced mudstone/wackestone. Aggradational parasequence has limy lithology and contains of these grain supported and mud supported facies. The base is dominated by big sub-aerial exposure and then followed by lagoonal shoal margin and ooid shoal setting. The upper part is dominated by low energy shallow subtidal to intertidal microbial flat.

Depositional units in KS1c

The base of this depositional sequence is dominated by mud supported facies and contains fenestral dolomudstone and ooid/bioclast dolowackestone to packstone. Appearance of lag deposits at the base shows start of a retrogradational parasequence. The maximum accommodation is indicated with dark gray shale interval and high stand system tracts with fining upward cycle, where fenestral mudstone reveals.

Overall, this unit represents a shallowing upward of the depositional system with intraclastic tidal channels, scours and transgressive lags at the base. The upper part of this unit, which is dominated by laminated dolomudstone is interpreted as intertidal mudflats and shallow lagoons and hyper saline lagoons.

Conclusion

The Dalan- Kangan carbonate rock units in the South Pars Gas Field contain the Permo-Triassic sequences of Iran. Based on a high resolution biostratigraphy, paleoenvironmental and sequence stratigraphy studies on this field, the Permian-Triassic boundary was identified precisely. The biostratigraphic studies led to identification of 95 species and 48 genera of benthic foraminifera and 6 species of algae based on which four biozones were erected for the Dalan Formation. These consist *Shanita amosi*, *Paraglobivalvulina mira*, *Paradagmarita monodi*, *Charliella altineri* with Late Midian, Early Djulfian, Middle Djulfian, and Late Djulfian ages, respectively. Also, the *Spirorbis phlyctaenae* biozone was recognized in the Kangan Formation indicating an age of Middle Triassic (Anisian) for this sector. The lack of schwagerinidea at the base of the Kangan Formation was an evidence for absence of the Mid Permian strata. The lack of *Colaniella* genus, the index fossil for the Late Permian strata in Tethys and Gondwana marginal basins, was another evidence for the Permian-Triassic disconformity. The *Spirorbis phlyctaenae* facies reported after mass extinction of Late Permian and thrombolite facies in this boundary are occurrences recorded between Dalan and Kangan formations generally indicating the lack of Late Permian (Dorashamian stage) and Early Triassic (Skythian stage) strata and confirming the disconformity at the boundary of Permian with Triassic.

In addition, eleven principal facies (MF) have been identified on the thin sections. These facies have been interpreted in terms of depositional environment including: 1) Sabkha (Supratidal/intertidal to subtidal setting), 2) Intertidal (intertidal to supratidal setting), 3) Lagoon (hyper saline to restricted lagoons), 4) leeward Shoals (lagoonal margin to lower intertidal setting), and 5) open marine (outer ramp setting, open marine muddy facies). However, from Dalan Formation through the Kangan Formation successions there are significant changes in platform type, facies organization and climate, consequently different depositional models presented for each of the major stratigraphic interval. Indeed, several depositional sequences have been identified, including:

KS4 and KS3 composite depositional sequence which are composed of two 3rd order cycles and are essentially transgressive in nature with a zone of maximum accommodation. KS2 is a 3rd order cycle, which is composed of grainy aggradational facies and local microbial mudstones. Finally, the KS1 is composite depositional sequence which includes three 3rd order cycles (KS1a, KS1b and KS1c).

The general paleogeographic context of this system was a marginal marine shelf setting with an inner platform that was very flat, ramp like, with little topography but with local depressions. The K1 unit is dominated by peritidal and evaporitic supratidal flats with pervasive microbial facies. This is also a zone of small shoal development. Therefore, most of these facies have seen in all the major Dalan and Kangan successions which their relative characteristics and distributions are not the same. However, from the K1 through to the K2 there have been significant changes in platform

sedimentation, facies associations and climate, consequently different depositional models presented for each of the major stratigraphic interval. The K2 is composed of grainy aggradational facies and local mudstones. The facies include beach and shallow water thrombolitic facies follow by storm generated pebble grainstone beds and shoals, which have variety degrees of microbial influence. The K3 is a system composed of restrictive coastal lagoons and shallow water muddy facies associated with some tongues of deepest parts of inner ramp facies. The K4 equates to huge subtidal bioclastic and oolithic shoals with local lagoons. It is mainly composed of bioclastic and oolitic transgressive sand wave complex which is preceded by a thin muddy open interval and finally capped by internal restricted platform conditions.

Acknowledgments
We thank PetroPars Company for kind permission to publish the manuscript, data preparation, and financial support.

Identified species in figure 4 are as follow:

1- *Hemigordiellina regularis*
2- *Midiella quinglogensis*
3- *Geinitzina ichnousa*
4- *Earlandia elegans*
5- *Agathammina pusilla*
6- *Geinitzina postcarbonica*
7- *Midiella* sp.
8- *Geinitzina* sp.
9- *Nankinella hunanensis*
10- *Glomomidiella nesteloroum*
11- *Hemigordius longus*
12- *Globivalvulina* sp.
13- *Globivalvulina bulloides*
14- *Globivalvulina graeca*
15- *Globivalvulina vonderschmitti*
16- *Chusenella abichi*
17- *Shanita amosi*
18- *Midiella zaninettiae*
19- *Nodosinelloides aequiampla*
20- *Nodosinelloides shikhanica*
21- *Cornuspira kinkelini*
22- *Tournayella moelleri*
23- *Nankinella minor*
24- *Hemigordiellina* sp.
25- *Agathammina subfusiformis*
26- *Baisalina pulchura*
27- *Glomomidiellopsis* sp.
28- *Hemigordius baoquingensis*
29- *Glomomidiella* sp.
30- *Earlandia* sp.
31- *Nodosinelloides* sp.
32- *Hemigordius* sp.
33- *Pseudoglomospira gordialiformis*
34- *Frondina permica*
35- *Globivalvulina cyprica*
36- *Sphaerulina croatica*
37- *Staffella yaziensis*
38- *Sphaerulina* sp.
39- *Glomospirella pseudopulchra*
40- *Baisalina* sp.
41- *Earlandia amplimuralis*
42- *Tournayella* sp.
43- *Earlandia vulgaris*
44- *Lasiodiscus tenuis*
45- *Earlandia minor*
46- *Agathammina ovata*
47- *Nankinella* sp.
48- *Neomillerella mirabilis*
49- *Midiella* aff. *Ovata*
50- *Neodiscopsis graecodisciformis ?*
51- *Pachyphloia* sp.
52- *Septaglobivalvulina* sp.
53- *Labiglobivalvulina fortis*
54- *Labiglobivalvulina* sp.
55- *Globivalvulina neglecta*
56- *Paraglobivalvulina mira*
57- *Paraglobivalvulina* sp.
58- *Globivalvulina nassichuki*
59- *Trepeilopsis minima*
60- *Polariisella* sp.
61- *Vicinesphaera* sp.
62- *Pachysphaera dervillei*
63- *Hoyenella hemigordiformis*
64- *Pachyphloia schwageri*
65- *Geinitzina* cf. *chapmani*
66- *Frondinodosaria* ? sp.
67- *Pachyphloia robusta*
68- *Pachyphloia ovata*
69- *Pachyphloia enormis*
70- *Colaniella* aff. *minuta*
71- *Dagmarita chanackchiensis*
72- *Langella massei* sp.
73- *Geinitzina reperta*
74- *Labiglobivalvulina baudi*

75- *Nodosinelloides mirabilis*
76- *Frondina* sp.
77- *Earlandia dunningtoni*
78- *Taurida nudiseptata*
79- *Paremiratella robusta*
80- *Archaediscus krestovnikovi*
81- *Hemigordius irregulariformis*
82- *Hemigordius schlumbergeri*
83- *Hemigordiopsis* sp.
84- *Ichthyofrondina* sp.
85- *Pachysphaera akkusica*
86- *Paradagmarita monodi*
87- *Ichthyolaria primitiva*
88- *Mediocris carinata*
89- *Pachysphaera polydermoides*
90- *Glomospirella ovalis*
91- *Mediocris* sp.
92- *Brunsispirella linae*
93- *Paraglobivalvulinoides septulifer*
94- *Charliella altineri*
95- *Spirorbis phlyctane*

References

Bronniman, F., Zaninetti, L., Bozorgnia, F., 1972. On the occurrence of Serpulid, Daudin, 1800 (Annelida, Polychaetia, Sedentarida) in the sections of Triassic rocks of Europe and Iran, Riv. Ital. Paleont, 78 (1): 67-90.

Dawson, O., Racey, A., Whittaker, J., 1993. The palaeoecological and palaeobiogepgraphic significance of Shanita (foraminifera) and associated foraminifera/algae from the Permian of peninsular Thailand; in T. Thanasuthipitak (Ed.), Proc. The BIOSEA Symposium, Chiang Mai University, Thiland, this volume.

Dawson, O., Pacey, A., Whittaker, J. E., 1994. Permian foraminifera from northeast and peninsular Thiland, Department of Geology, University of London, Egham, Survey TW20 0EX, U.K.

Ehrenberg, S. N., 2007. Porosity destruction in carbonate platforms. J. Pet. Geol, 29: 41–52.

Flugel, E., 2004. Microfacies of Carbonate Rocks, Springer-Verlag, Berlin.

Gaillot, J., Vachard, D., 2007. The Khuff Formation (Middle East) and time equivalents in Turkey and South China: biostratigraphy from Capitanian to Changhsingian times (Permian), new foraminiferal taxa, and palaeogeographical implications. Journal of Coloquios de Paleontología, 57: 37-223.

Gaillot, J., Vachard, D., Galfetti, Th., Martini, R., 2009. New latest Permian foraminifers from Laren (Guangxi Province, South China): Palaeobiogeographic implications, Journal of Geobios, 42: 141–168.

Grotzinger, J. P., 2000. Facies and paleoenvironmental setting of thrombolite-stromatolite reefs, terminal Proterozoic Nama Group (ca. 550–543 Ma), central and southern Namibia. Communications of the Geological Survey of Namibia, 12: 221-233.

Groves, J. R., D., Altiner, R., 2005. Extinction, survival, and recovery of Lagenide foraminifers in the Permian Triassic boundary interval, Central Taurides, Turkey: The Paleontological Society Memoir 62, Suppl. to J. Paleontol, 79 (4): 1–38.

Insalaco, E., A., Virgone, B., Courme, J., Gaillote, S., A., Kamali, M., R., Moallemi, M., Lotfpour, S., Monibi., 2006. Upper Dalan member and Kangan Formation between the Zagros mountains and offshore Fars, Iran: depositional system, biostratigraphy and stratigraphic architecture: Journal of Geo Arabia, 11: 75-176.

Kashfi, M. S., 2000. Greater Persian Gulf Permian–Triassic stratigraphic nomenclature requires study. Oil and Gas Journal, 6: 36–44.

Koehrer, B., Zeller, M., Aigner, T., Poeppelreiter, M., Milroy, P., Forke, H., Al-Kindi, S., 2010. Facies and stratigraphic framework of a Khuff outcrop equivalent: Saiq and Mahil formations, Al Jabal al-Akhdar, Sultanate of Oman, Journal of GeoArabia, 15 (2): 91-156.

Kolodka, C., Vennin, E., Vachard, D., Trocme, V., Goodarzi, M. H., 2011. Timing and progression of the end-Guadalupian crisis in the Fars province (Dalan Formation, Kuh-e Gakhum, Iran) constrained by foraminifers and other carbonate microfossils, Journal of Facies, DOI 10.1007/s10347-011-0265-1.

Krainer, K., Vachard, D., 2011. The Lower Triassic Werfen Formation of the Karawanken Mountains (Southern Austria) and its disaster survivor microfossils, with emphasis on Postcladella n. gen. (Foraminifera, Miliolata, Cornuspirida), Journal of Revue de micropaléontologie, 54: 59-85.

Leven, E. Ya., 1991. Pervyenakhoki v SSSR foraminifer rodashanita (semeistvoHemigordiopsidae) [Firt discovery in USSR of the foraminifer genus Shanita (family Hemigordiopsidae). Paleontologiskii Zhurnal, 2: 102-104 (in Russian).

Lys, M., Stampfli, G., Jenny, J., 1978. Biostratigraphie du Carbonife're et du Permien de l'Elbourz oriental (Iran du NE), Note Labor. Paleont. Univ. Gene've, 10: 63-100.

Mohtat-Aghai, P., Vachard., D., 2005. Late Permian foraminiferal assemblages from the Hambast region (Central Iran) and their extinctions. Revista Espanola de Micropaleontologia, 37 (2): 205-227.

Rahimpour-Bonab, H., Asadi-Eskandar, A., Sonei, A., 2009. Controls of Permian-Triassic Boundary over Reservoir Characteristics of South Pars Gas Field, Persian Gulf. Geol. J, 44: 341–364.

Schubert, J. K., D. J., Bottjer., 1992. Early Triassic stromatolites as post mass extinction disaster forms: Geology, 20 (10): 883–886.

Sharland, P. R., Archer, R., Casey, D. M., Davies, R. B., Hall, S. H., Heward, A. P., Horbury, A. D., Simmons, M. D., 2001. Arabian Plate Sequence Stratigraphy. GeoArabia Special Publication, 2: 1–371.

Song, H., J., Tong, J., N., Zhang K., X., Wang Q., X., Chen, Z. Q., 2007. Foraminiferal survivors from the Permian-Triassic mass extinction in the Meishan section, South China, Journal of Palaeoworld, 16: 105-119.

Song, H., Tong, J., Chen, Z. Q., 2011. Evolutionary dynamics of the Permian-Triassic foraminifer size: Evidence for Lilliput effect in the End-Permian mass extinction and its aftermath, Journal of Palaeogeography, Palaeoclimatology, Palaeoecology, 308: 98-110.

Stampfly, G. M., 2000. Tethyan oceans. In: Tectonics and Magmatism in Turkey and the Surrounding Area. Bozkurt, E., Winchester, J. A., Piper, J. D. A., Eds., Geological Society of London, Special Publications, 173: 1-23.

Stanley, S. M., X., Yang., 1994. A double mass extinction at the end of the Paleozoic era: Science, 266 (5189): 1340-1344.

Szabo, F., Keradpir, A., 1978. Permian and Triassic stratigraphy Zagros Basin, Southwest Iran. J. Petrol. Geol, 1: 57–82.

Vachard, D., Pille, L., Gaillot, J., 2010. Palaeozoic Foraminifera: Systematics, palaeoecology and responses to global changes, Journal of revue de micropaleontology, 53: 209-254.

Wignall, P. B., Hallam, A., 1992. Anoxia as a cause of the Permian–Triassic mass extinction: facies evidence from northern Italy. Palaeogeography, Palaeoclimatology, Palaeoecology, 93: 21–46.